

# A limit on the mass of the $\nu_\tau$

CLEO Collaboration

R. Ammar <sup>a</sup>, P. Baringer <sup>a</sup>, A. Bean <sup>a</sup>, D. Besson <sup>a</sup>, D. Coppage <sup>a</sup>, C. Darling <sup>a</sup>,  
R. Davis <sup>a</sup>, S. Kotov <sup>a</sup>, I. Kravchenko <sup>a</sup>, N. Kwak <sup>a</sup>, L. Zhou <sup>a</sup>, S. Anderson <sup>b</sup>,  
Y. Kubota <sup>b</sup>, S.J. Lee <sup>b</sup>, J.J. O'Neill <sup>b</sup>, R. Poling <sup>b</sup>, T. Riehle <sup>b</sup>, A. Smith <sup>b</sup>,  
M.S. Alam <sup>c</sup>, S.B. Athar <sup>c</sup>, Z. Ling <sup>c</sup>, A.H. Mahmood <sup>c</sup>, S. Timm <sup>c</sup>, F. Wappler <sup>c</sup>,  
A. Anastassov <sup>d</sup>, J.E. Duboscq <sup>d</sup>, D. Fujino <sup>d,1</sup>, K.K. Gan <sup>d</sup>, T. Hart <sup>d</sup>,  
K. Honscheid <sup>d</sup>, H. Kagan <sup>d</sup>, R. Kass <sup>d</sup>, J. Lee <sup>d</sup>, H. Schwarthoff <sup>d</sup>, M.B. Spencer <sup>d</sup>,  
M. Sung <sup>d</sup>, A. Undrus <sup>d,2</sup>, A. Wolf <sup>d</sup>, M.M. Zoeller <sup>d</sup>, S.J. Richichi <sup>e</sup>, H. Severini <sup>e</sup>,  
P. Skubic <sup>e</sup>, M. Bishai <sup>f</sup>, J. Fast <sup>f</sup>, J.W. Hinson <sup>f</sup>, N. Menon <sup>f</sup>, D.H. Miller <sup>f</sup>,  
E.I. Shibata <sup>f</sup>, I.P.J. Shipsey <sup>f</sup>, M. Yurko <sup>f</sup>, S. Glenn <sup>g</sup>, Y. Kwon <sup>g,3</sup>, A.L. Lyon <sup>g</sup>,  
S. Roberts <sup>g</sup>, E.H. Thorndike <sup>g</sup>, C.P. Jessop <sup>h</sup>, K. Lingel <sup>h</sup>, H. Marsiske <sup>h</sup>,  
M.L. Perl <sup>h</sup>, V. Savinov <sup>h</sup>, D. Ugolini <sup>h</sup>, X. Zhou <sup>h</sup>, T.E. Coan <sup>i</sup>, V. Fadeyev <sup>i</sup>,  
I. Korolkov <sup>i</sup>, Y. Maravin <sup>i</sup>, I. Narsky <sup>i</sup>, V. Shelkov <sup>i</sup>, J. Staeck <sup>i</sup>, R. Stroynowski <sup>i</sup>,  
I. Volobouev <sup>i</sup>, J. Ye <sup>i</sup>, M. Artuso <sup>j</sup>, F. Azfar <sup>j</sup>, A. Efimov <sup>j</sup>, M. Goldberg <sup>j</sup>, D. He <sup>j</sup>,  
S. Kopp <sup>j</sup>, G.C. Moneti <sup>j</sup>, R. Mountain <sup>j</sup>, S. Schuh <sup>j</sup>, T. Skwarnicki <sup>j</sup>, S. Stone <sup>j</sup>,  
G. Viehhauser <sup>j</sup>, J.C. Wang <sup>j</sup>, X. Xing <sup>j</sup>, J. Bartelt <sup>k</sup>, S.E. Csorna <sup>k</sup>, V. Jain <sup>k,4</sup>,  
K.W. McLean <sup>k</sup>, S. Marka <sup>k</sup>, R. Godang <sup>l</sup>, K. Kinoshita <sup>l</sup>, I.C. Lai <sup>l</sup>,  
P. Pomianowski <sup>l</sup>, S. Schrenk <sup>l</sup>, G. Bonvicini <sup>m</sup>, D. Cinabro <sup>m</sup>, R. Greene <sup>m</sup>,  
L.P. Perera <sup>m</sup>, G.J. Zhou <sup>m</sup>, M. Chadha <sup>n</sup>, S. Chan <sup>n</sup>, G. Eigen <sup>n</sup>, J.S. Miller <sup>n</sup>,  
M. Schmidtler <sup>n</sup>, J. Urheim <sup>n</sup>, A.J. Weinstein <sup>n</sup>, F. Würthwein <sup>n</sup>, D.W. Bliss <sup>o</sup>,  
D.E. Jaffe <sup>o</sup>, G. Masek <sup>o</sup>, H.P. Paar <sup>o</sup>, S. Prell <sup>o</sup>, V. Sharma <sup>o</sup>, D.M. Asner <sup>p</sup>,  
J. Gronberg <sup>p</sup>, T.S. Hill <sup>p</sup>, D.J. Lange <sup>p</sup>, R.J. Morrison <sup>p</sup>, H.N. Nelson <sup>p</sup>,  
T.K. Nelson <sup>p</sup>, D. Roberts <sup>p</sup>, B.H. Behrens <sup>q</sup>, W.T. Ford <sup>q</sup>, A. Gritsan <sup>q</sup>, J. Roy <sup>q</sup>,  
J.G. Smith <sup>q</sup>, J.P. Alexander <sup>r</sup>, R. Baker <sup>r</sup>, C. Bebek <sup>r</sup>, B.E. Berger <sup>r</sup>, K. Berkelman <sup>r</sup>,  
K. Bloom <sup>r</sup>, V. Boisvert <sup>r</sup>, D.G. Cassel <sup>r</sup>, D.S. Crowcroft <sup>r</sup>, M. Dickson <sup>r</sup>,  
S. von Dombrowski <sup>r</sup>, P.S. Drell <sup>r</sup>, K.M. Ecklund <sup>r</sup>, R. Ehrlich <sup>r</sup>, A.D. Foland <sup>r</sup>,  
P. Gaidarev <sup>r</sup>, L. Gibbons <sup>r</sup>, B. Gittelman <sup>r</sup>, S.W. Gray <sup>r</sup>, D.L. Hartill <sup>r</sup>,  
B.K. Heltsley <sup>r</sup>, P.I. Hopman <sup>r</sup>, J. Kandaswamy <sup>r</sup>, D.L. Kreinick <sup>r</sup>, T. Lee <sup>r</sup>, Y. Liu <sup>r</sup>,  
N.B. Mistry <sup>r</sup>, C.R. Ng <sup>r</sup>, E. Nordberg <sup>r</sup>, M. Ogg <sup>r,5</sup>, J.R. Patterson <sup>r</sup>, D. Peterson <sup>r</sup>,

D. Riley <sup>r</sup>, A. Soffer <sup>r</sup>, B. Valant-Spaight <sup>r</sup>, C. Ward <sup>r</sup>, M. Athanas <sup>s</sup>, P. Avery <sup>s</sup>,  
 C.D. Jones <sup>s</sup>, M. Lohner <sup>s</sup>, S. Patton <sup>s</sup>, C. Prescott <sup>s</sup>, J. Yelton <sup>s</sup>, J. Zheng <sup>s</sup>,  
 G. Brandenburg <sup>t</sup>, R.A. Briere <sup>t</sup>, A. Ershov <sup>t</sup>, Y.S. Gao <sup>t</sup>, D.Y.-J. Kim <sup>t</sup>,  
 R. Wilson <sup>t</sup>, H. Yamamoto <sup>t</sup>, T.E. Browder <sup>u</sup>, Y. Li <sup>u</sup>, J.L. Rodriguez <sup>u</sup>,  
 T. Bergfeld <sup>v</sup>, B.I. Eisenstein <sup>v</sup>, J. Ernst <sup>v</sup>, G.E. Gladding <sup>v</sup>, G.D. Gollin <sup>v</sup>,  
 R.M. Hans <sup>v</sup>, E. Johnson <sup>v</sup>, I. Karliner <sup>v</sup>, M.A. Marsh <sup>v</sup>, M. Palmer <sup>v</sup>, M. Selen <sup>v</sup>,  
 J.J. Thaler <sup>v</sup>, K.W. Edwards <sup>w</sup>, A. Bellerive <sup>x</sup>, R. Janicek <sup>x</sup>, D.B. MacFarlane <sup>x</sup>,  
 P.M. Patel <sup>x</sup>, A.J. Sadoff <sup>y</sup>

<sup>a</sup> University of Kansas, Lawrence, KS 66045, USA

<sup>b</sup> University of Minnesota, Minneapolis, MN 55455, USA

<sup>c</sup> State University of New York at Albany, Albany, NY 12222, USA

<sup>d</sup> Ohio State University, Columbus, OH 43210, USA

<sup>e</sup> University of Oklahoma, Norman, OK 73019, USA

<sup>f</sup> Purdue University, West Lafayette, IN 47907, USA

<sup>g</sup> University of Rochester, Rochester, NY 14627, USA

<sup>h</sup> Stanford Linear Accelerator Center, Stanford University, Stanford, CA 94309, USA

<sup>i</sup> Southern Methodist University, Dallas, TX 75275, USA

<sup>j</sup> Syracuse University, Syracuse, NY 13244, USA

<sup>k</sup> Vanderbilt University, Nashville, TN 37235, USA

<sup>l</sup> Virginia Polytechnic Institute and State University, Blacksburg, VA 24061, USA

<sup>m</sup> Wayne State University, Detroit, MI 48202, USA

<sup>n</sup> California Institute of Technology, Pasadena, CA 91125, USA

<sup>o</sup> University of California, San Diego, La Jolla, CA 92093, USA

<sup>p</sup> University of California, Santa Barbara, CA 93106, USA

<sup>q</sup> University of Colorado, Boulder, CO 80309-0390, USA

<sup>r</sup> Cornell University, Ithaca, NY 14853, USA

<sup>s</sup> University of Florida, Gainesville, FL 32611, USA

<sup>t</sup> Harvard University, Cambridge, MA 02138, USA

<sup>u</sup> University of Hawaii at Manoa, Honolulu, HI 96822, USA

<sup>v</sup> University of Illinois, Urbana-Champaign, IL 61801, USA

<sup>w</sup> Carleton University, Ottawa, Ont. K1S 5B6, Canada

and the Institute of Particle Physics, Canada

<sup>x</sup> McGill University, Montréal, Que. H3A 2T8, Canada

and the Institute of Particle Physics, Canada

<sup>y</sup> Ithaca College, Ithaca, NY 14850, USA

Received 3 April 1998

Editor: L. Montanet

---

## Abstract

A limit on the mass of the tau neutrino  $m_{\nu_\tau}$  is derived from  $4.5 \times 10^6$  tau pairs produced in an integrated luminosity of  $5.0 \text{ fb}^{-1}$  of  $e^+e^- \rightarrow \gamma^* \rightarrow \tau^+\tau^-$  reactions at center of mass energies  $\approx 10.6 \text{ GeV}$ . The measurement technique involves a two-dimensional extended likelihood analysis, including the dependence of the end-point population on  $m_{\nu_\tau}$ , and allows for the first time an explicit background contribution. We use the decays  $\tau \rightarrow 5\pi\nu_\tau$  and  $\tau \rightarrow 3\pi 2\pi^0\nu_\tau$  to obtain an upper limit of  $30 \text{ MeV}/c^2$  at 95% C.L. © 1998 Elsevier Science B.V. All rights reserved.

PACS: 14.60.Lm; 12.15.Ff; 13.35.Dx

Keywords: Tau neutrino mass

---

Although the tau neutrino has never been directly observed, the question of its mass is an important issue in particle physics and cosmology. While the requirement that the density of primordial relic neutrinos from the Big Bang not over-close the Universe restricts the mass of a stable neutrino to be less than  $\sim 100 \text{ eV}/c^2$  [1–5], unstable neutrinos are less restricted. Big Bang nucleosynthesis models allow for a massive neutrino in the 10 to 31  $\text{MeV}/c^2$  range for lifetimes in the 0.01 to 40 second interval [6]<sup>6</sup>. This astrophysically allowed range currently overlaps the experimentally accessible bounds. The most stringent accelerator-based limits on  $m_{\nu_\tau}$  are derived from one-dimensional mass fits and two-dimensional energy versus mass fits of the hadrons in tau decays. The sensitivity of the method is largest when the invariant hadronic mass is large, and there is little phase space for the (unseen) neutrino such as in the decays modes  $\tau \rightarrow 5\pi(\pi^0)\nu_\tau$  and  $\tau \rightarrow 3\pi 2\pi^0\nu_\tau$ . In addition, due to its large branching ratio, the decay  $\tau \rightarrow 3\pi\nu_\tau$  can be used in spite of its lower inherent sensitivity per event resulting from its low average hadronic decay product mass.

The lowest published upper limit<sup>7</sup>, by the ALEPH collaboration [8], is  $24 \text{ MeV}/c^2$  and is obtained with a two-dimensional likelihood fit to a region near the endpoint of  $25 \ 5\pi(\pi^0)$  candidate events. By doubling this dataset and adding in  $3\pi$  decay candidates, the ALEPH collaboration [9] has recently reported an upper limit of  $18.2 \text{ MeV}/c^2$ . The DELPHI collaboration [10] has claimed a limit of  $33 \text{ MeV}/c^2$  in the  $3\pi$  mode from a mass fit, but notes that this limit is sensitive to the contribution of a possible higher mass resonance in the  $3\pi$  mass distribution. DELPHI estimates that the model dependence in the  $3\pi$  mode increases the limit to  $62 \text{ MeV}/c^2$ . The OPAL collaboration [11] quotes a  $35.3 \text{ MeV}/c^2$  limit from a two-dimensional fit to the missing momentum and missing mass in  $3\pi$  decays using the event thrust axis as an estimator of the tau direction. Combining this with an earlier limit of  $74 \text{ MeV}/c^2$  from  $5\pi$  decays [12], a  $29.9 \text{ MeV}/c^2$  limit is obtained. ARGUS [13,14] has published a  $31 \text{ MeV}/c^2$  limit based on a one-dimensional mass fit to 20  $5\pi$  events. The previous CLEO limit [15] of  $32.6 \text{ MeV}/c^2$  was set with a fit to the mass spectrum of 60  $5\pi$  events, and 53  $3\pi 2\pi^0$  events.

The current analysis uses data collected with the CLEO II detector [16] at the Cornell  $e^+e^-$  storage ring (CESR) at center of mass energies near 10.6 GeV. The data set consists of  $5.0 \text{ fb}^{-1}$  of integrated luminosity corresponding to 4.5 million produced tau pairs. The tau's, created mainly via  $e^+e^- \rightarrow \gamma^* \rightarrow \tau^+\tau^-$ , have the full beam energy of 5.29 GeV and recoil back to back, modulo initial state radiation effects. The decay modes studied are  $\tau \rightarrow 5\pi\nu_\tau$  and  $\tau \rightarrow 3\pi 2\pi^0\nu_\tau$  recoiling against a leptonically-decaying tau (the “tag”). An upper limit on  $m_{\nu_\tau}$  is obtained from a two-dimensional likelihood fit to hadronic mass and energy in these decays. The likelihood includes for the first time a background contribution, as well as a factor describing the expected number of events as a function of neutrino mass, and measured event errors for hadronic mass and energy.

In order to avoid a spuriously low limit from a background event, the event selection criteria are chosen to obtain a very pure event sample of  $\tau \rightarrow 5\pi\nu_\tau$  or  $3\pi 2\pi^0\nu_\tau$ , and roughly follow those of our last publication [15]. A clean sample of tau's is obtained by selecting events in which the tag decays leptonically:  $\tau \rightarrow e\nu_\tau$  or  $\tau \rightarrow \mu\nu_\tau$ . We thus require the event to contain an isolated lepton ( $e$  or  $\mu$ ) in the barrel ( $|\cos\theta| < 0.71$ ) recoiling against 5 or 3 charged tracks, with event hemispheres defined by the event thrust axis. Exactly 6 or 4 charged tracks consistent with production at the nominal interaction point are required, after pairs of tracks consistent with photon conversions and Dalitz  $\pi^0$  or  $K_S^0$  decays are rejected. Backgrounds from two photon events are minimized by requiring that the total missing momentum point away from the beamline, and that the total energy transverse to the beam axis be above 200 MeV. To suppress hadronic events, the total visible energy is required to be below 90% of the total center of mass energy. All hadronic tracks must also have a specific

<sup>1</sup> Permanent address: Lawrence Livermore National Laboratory, Livermore, CA 94551.

<sup>2</sup> Permanent address: BINP, RU-630090 Novosibirsk, Russia.

<sup>3</sup> Permanent address: Yonsei University, Seoul 120-749, Korea.

<sup>4</sup> Permanent address: Brookhaven National Laboratory, Upton, NY 11973.

<sup>5</sup> Permanent address: University of Texas, Austin TX 78712.

<sup>6</sup> Recently [7] it has been pointed out that these arguments do depend upon which set of astrophysical observations are used.

<sup>7</sup> All neutrino mass upper limits quoted herein are at the 95% confidence level.

ionization ( $dE/dx$ ) consistent with that of a pion. We correct for  $dE/dx$  energy loss when computing energies and invariant masses.

Isolated showers in the calorimeter with photon-like lateral shower profiles are identified as photons. In the barrel, photon candidates must have an energy above 60 MeV, while in the range  $0.71 < |\cos \theta| < 0.95$ , they must have an energy above 100 MeV. Exactly 0 or 2 neutral pions must be reconstructed on the signal side, with none on the tag side. These  $\pi^0$  candidates must have an opening angle of less than  $60^\circ$  and a mass constrained fit of the  $\pi^0$  candidates must have a confidence level greater than 5%. If the photon candidates can be combined into  $\pi^0$ s in multiple ways, we select the combination with the smallest total  $\chi^2$  for the  $\pi^0$  mass hypothesis. We permit calorimeter showers that are unassociated with charged tracks or  $\pi^0$ s to remain. The summed energy of all showers within  $90^\circ$  of the lepton direction must be less than 100 MeV in each of the barrel and endcap region of the calorimeter. For the signal hemisphere, the energy requirement is increased to 200 MeV.

The selection criteria above were designed to minimize backgrounds, which arise primarily from non-tau decays such as  $e^+e^- \rightarrow q\bar{q}$  or  $e^+e^- \rightarrow T(4S) \rightarrow B\bar{B}$  or from feedthrough from other tau decay modes. A data sample which satisfies the above selection criteria on the signal side of the event, but with an invariant mass above the tau mass on the tag side, is used as an estimator of non-tau backgrounds. The background estimate is obtained by scaling the number of these estimator events above the tau mass on the signal side to the number of data events above the tau mass on the signal side minus the Monte Carlo predicted number of taus misreconstructed above the tau mass. The background estimates obtained in this way are consistent with those obtained by using  $e^+e^- \rightarrow q\bar{q}$  Lund [17] generated Monte Carlo events. Monte Carlo events with full detector simulation [18] based on the event generators KORALB [19] and PHOTOS [20] were used to estimate tau decay backgrounds in the signal hemisphere (feed-across).

The resulting event distributions, shown in Fig. 1, contain 266 events in the  $5\pi$  final state, of which 8 are above the tau mass. The  $3\pi 2\pi^0$  mode contains 207 events, of which 13 are above the tau mass. Monte Carlo simulations show a reconstruction efficiency of  $(3.08 \pm 0.10)\%$  for the  $5\pi$  mode and  $(0.43 \pm 0.02)\%$  for the  $3\pi 2\pi^0$  mode. In both modes the number of events observed is consistent with the expectation from the world average branching fractions [21].

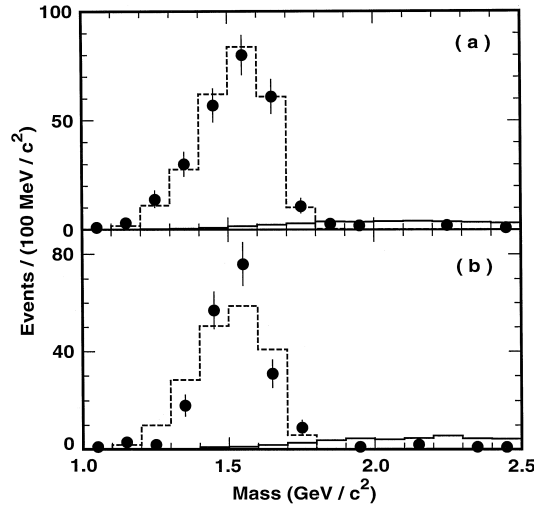


Fig. 1. The mass distributions of the  $5\pi$  (a) and  $3\pi 2\pi^0$  (b) data samples. The dashed histogram represents the shape expected from Monte Carlo normalized to the number of events below the tau mass. The background estimate is shown as a solid histogram and is normalized for display purposes to five times its nominal value.

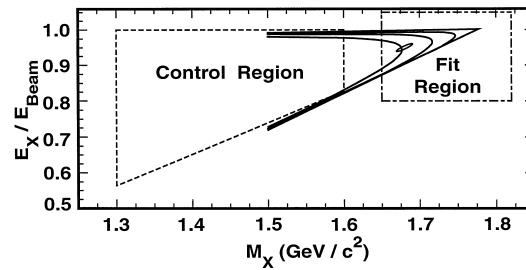


Fig. 2. The number of events in the the fit region  $\Omega$  relative to the number in the control region  $\mathcal{R}$  in the scaled hadronic energy versus hadronic mass plane is a function of neutrino mass. Kinematically allowed neutrino mass contours are drawn for neutrino masses of 0, 30, 60 and 100  $\text{MeV}/c^2$ . Note the typical error ellipse drawn in the fit region.

Each signal event is represented by a point in the two-dimensional plane formed by the hadronic energy scaled to the beam energy ( $E_X/E_B$ ) versus hadronic mass ( $M_X$ ), with the estimated errors represented by an ellipse. The sensitivity to neutrino mass is largest in the region near  $M_X = m_\tau$  and  $E_X/E_B = 1$ , as shown in Fig. 2. The data events are shown in Fig. 3. We determine the tau neutrino mass using the events lying in the fit region  $\Omega$  shown in Fig. 2. There are 36  $5\pi$  events in the fit region, with negligible tau backgrounds and an estimated 0.3 events from non-tau backgrounds. There are 19  $3\pi 2\pi^0$  events in the fit region, with 1.0 of these expected as feed-across from other tau decay modes and 0.4 expected from non-tau backgrounds. Details of the analysis are summarized in Table 1.

We extract a measurement of the tau neutrino mass using an unbinned extended maximum likelihood technique. The procedure fits for one parameter ( $m_\nu$ ), taking as input the measured hadronic energy and mass of the events in the fit region shown in Fig. 2. The likelihood function, detailed in the appendix, is composed of a Poisson factor, expressing the number of events expected, times the sum of a signal term and a background term. The likelihood is calculated as a function of neutrino mass using a novel technique. Instead of using

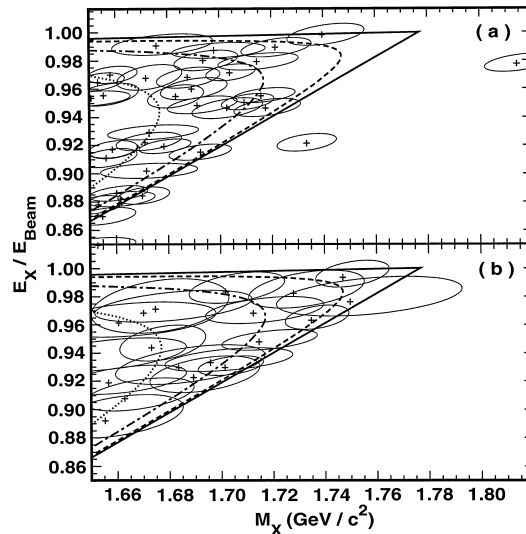


Fig. 3. The hadronic scaled energy versus mass distribution of the  $5\pi$  (a) and  $3\pi 2\pi^0$  (b) data samples in the fit region. Ellipses represent  $1\sigma$  resolution errors and incorporate reconstruction induced systematic offsets. Kinematically allowed contours are drawn for neutrino masses of 0, 30, 60 and 100  $\text{MeV}/c^2$  as solid, dashed, dot-dashed and dotted lines respectively. Events below the kinematically allowed region are fully consistent with signal events, once initial state radiation effects are considered (as they are in the likelihood.)

Table 1

Summary of signal, background, efficiency, resolution and upper limit by mode

Mode	$5\pi$	$3\pi 2\pi^0$
Total Events	266	207
Events in Fit Region	36	19
Signal Region Purity (%)	99	93
Selection Efficiency (%)	3.08	0.43
Typical Mass Resolution ( $\text{MeV}/c^2$ )	15	25
Typical Energy Resolution ( $\text{MeV}$ )	25	50
Upper Limit @ 95 % CL ( $\text{MeV}/c^2$ )	31	33

explicit parameterizations of the Monte Carlo in a likelihood convolution [22], Monte Carlo signal events are used in the evaluation of the likelihood, directly implementing the best knowledge of all physics effects including initial state radiation and detector acceptance. The only explicitly parameterized term is the detector smearing function.

The resulting extended likelihood is shown in Fig. 4. We define <sup>8</sup> the 95% confidence level (CL) upper limit by integrating defined likelihood above zero mass to its ninety-fifth percentile. We find 95% CL upper limits of 33, 31, and 27  $\text{MeV}/c^2$  for the  $3\pi 2\pi^0$ ,  $5\pi$  and combined samples. A separate analysis using only mass information yields a combined upper limit of 31  $\text{MeV}/c^2$ .

The interpretation of this limit as a meaningful statement about probability is conditional upon the measured likelihood being representative of an ensemble of similar experiments. The event distribution and the observed number of events at the endpoint are consistent with our Monte Carlo estimation with zero neutrino mass, using the spectral function tuned to the data as described below. An ensemble of Monte Carlo experiments using statistics compatible with those we observe reveal that a smaller upper limit is obtained in 67% of experiments with a massless neutrino. The average expected upper limit given our sample size is found to be 25  $\text{MeV}/c^2$ .

Following the conservative prescription used by the LEP experiments [22], a linear systematic error,  $\Delta(m_{95})$ , is added to the limit. The error is defined by

$$\Delta(m_{95})^2 = \Sigma (\tilde{m}_{95} - m_{95})^2,$$

where the sum is over systematic error sources, and the difference represents the change in the nominal upper limit from each error source. Systematic errors are summarized in Table 2.

The largest systematic error is due to uncertainties in the spectral functions. We obtain the spectral functions from a fit to a statistically independent sample of decays recoiling against pionic decays of the tau, excluding the 100  $\text{MeV}/c^2$  near the tau mass and including a background term. Each fit is a sum of two phenomenologically inspired spectra [23–25]; the dominant spectrum is the distribution predicted for the 5 pion decay of the tau as derived from the CVC predictions for 4 pion decay and soft pion theorems, and the other is the harder spectrum CVC predicts for 6 pion decays. The systematic variation for the spectral function is taken as the allowed variation in the fit parameters and results in errors of 1.5  $\text{MeV}/c^2$  from the  $5\pi$  mode and 1.1  $\text{MeV}/c^2$  from the  $3\pi 2\pi^0$  mode.

The next largest systematic error comes from the modeling of the detector smearing function. The smearing function is approximated by a sum of three two-dimensional Gaussians to model its extended tails. The smearing function parameters are derived from the Monte Carlo simulation, while the widths of each Gaussian are proportional to the event error, as estimated from the propagated tracking error matrix and the photon

<sup>8</sup> The method for extracting an upper limit from a likelihood distribution at a given confidence level is not unambiguously defined; the method used here differs from that used in the analysis of Ref. [8]. Therefore comparisons of upper limits among different experiments must be done with care.

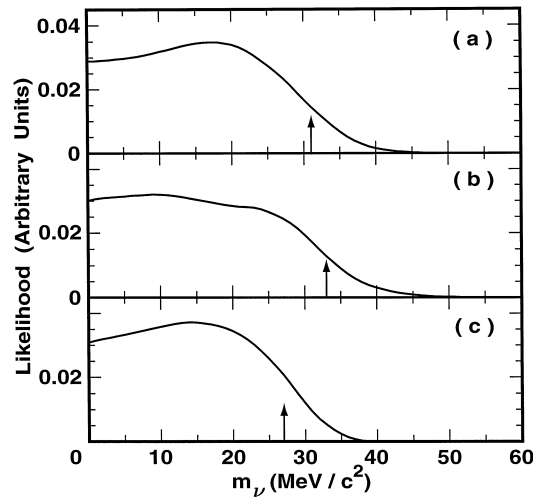


Fig. 4. The likelihood as a function of neutrino mass for the  $5\pi$  (a),  $3\pi 2\pi^0$  (b) and combined (c) data samples. The 95% CL upper limits, uncorrected for systematic errors, are at 31, 33, and 27  $\text{MeV}/c^2$ , respectively.

reconstruction errors. The errors from the modeling of the tails of the smearing function are estimated by using a fourth Gaussian component in separate fits to charm and  $B$  decay data. The mass (energy) smearing is studied with charm ( $B$ ) decays to final states with similar numbers of tracks as our samples.  $B$  decays are used since the  $B$ , created nearly at rest in the CLEO detector frame, allows the comparison of reconstructed energy with the beam energy. This smearing uncertainty is  $1.4 \text{ MeV}/c^2$  for the  $3\pi 2\pi^0$  mode and  $0.6 \text{ MeV}/c^2$  for the  $5\pi$  mode. In addition, all smearing function parameters are allowed to vary within their fitted uncertainties, resulting in another  $0.5 \text{ MeV}/c^2$  uncertainty for each of the two modes.

The uncertainty in the absolute mass and energy scales of  $1 \text{ MeV}/c^2$  (as estimated from charm decays) and  $2.7 \text{ MeV}$  (from  $B$  decays), respectively, contribute  $1.1 \text{ MeV}/c^2$  and  $0.3 \text{ MeV}/c^2$  to the final systematic error estimate.

Other sources of error considered are the Monte Carlo statistics used in the likelihood evaluation and the background size. The total systematic error from all sources added in quadrature is  $2.9 \text{ MeV}/c^2$ , resulting in a final 95% C.L. upper limit on the mass of the tau neutrino of  $30 \text{ MeV}/c^2$ .

The use of the Poisson term in this analysis' likelihood is an improvement over a previous technique [8] because it reduces the variance in fitted neutrino mass, thus decreasing the probability of a spuriously low limit in the presence of a massive neutrino. The present analysis also uses measured event errors to avoid a possible

Table 2  
Systematic error summary

Source	Error ( $\text{MeV}/c^2$ )
Spectral Function	1.9
Smearing Tails	1.6
Mass Scale	1.1
Smearing Parameters	0.7
MC Statistics	0.6
Background	0.4
Energy Scale	0.3
Total	2.9

bias. The smearing shape used in previous analyses [8,12] depends on repeated Monte Carlo simulation of the data points, using the measured values as input to the Monte Carlo event generator. Such a method neglects the fact that events reconstructed near the endpoint stand a larger chance of being upward fluctuations from low mass events than do events in the middle of the accepted distribution, and thus tends to underestimate the mass and energy errors associated with each data point.

In summary, using the world's largest sample of candidate  $\tau \rightarrow 5\pi\nu_\tau$  and  $\tau \rightarrow 3\pi 2\pi^0\nu_\tau$  decays, we obtain a 95% confidence level upper limit on  $m_{\nu_\tau}$  of 30 MeV/ $c^2$ . The method used properly takes into account the change in the number of events expected at the endpoint as a function of  $m_{\nu_\tau}$ , as well as a background contribution, and a detailed detector smearing function.

## Acknowledgements

We gratefully acknowledge the effort of the CESR staff in providing us with excellent luminosity and running conditions. J.R. Patterson and I.P.J. Shipsey thank the NYI program of the NSF, M. Selen thanks the PFF program of the NSF, M. Selen and H. Yamamoto thank the OJI program of DOE, J.R. Patterson, K. Honscheid, M. Selen and V. Sharma thank the A.P. Sloan Foundation, M. Selen thanks Research Corporation, S. von Dombrowski thanks the Swiss National Science Foundation, and H. Schwarthoff thanks the Alexander von Humboldt Stiftung for support. This work was supported by the National Science Foundation, the US Department of Energy, and the Natural Sciences and Engineering Research Council of Canada.

## Appendix A

The likelihood is given by

$$\mathcal{L}(m_\nu) = \mathcal{P}(N_{\text{obs}}) \prod_{\text{Events}} \mathcal{L}_{\text{dat}}(\tilde{X}_{\text{data}} | \sigma_{\text{data}}, m_\nu, \bar{N}_{\text{bgd}}).$$

The first factor is the Poisson probability of the number of events observed in the fit region,  $N_{\text{obs}}$ . The second factor is the product likelihood over the data events observed  $\tilde{X}_{\text{data}}$ , and their associated errors  $\sigma_{\text{data}}$ , given an expected number of background events,  $\bar{N}_{\text{bgd}}$ .

The Poisson factor is

$$\mathcal{P}(N_{\text{obs}}) = (\bar{N}(m_\nu) + \bar{N}_{\text{bgd}})^{N_{\text{obs}}} \left[ \frac{e^{-(\bar{N}(m_\nu) + \bar{N}_{\text{bgd}})}}{N_{\text{obs}}!} \right].$$

The expected number of signal events in the fit region  $\Omega$ ,  $\bar{N}(m_\nu)$ , is a function of neutrino mass and is extrapolated from the number of events seen in the control region  $\mathcal{R}$  using the partial width

$$\bar{N}(m_\nu) = \frac{\int_{\Omega} d\Gamma(m_\nu)}{\int_{\mathcal{R}} d\Gamma(m_\nu = 0)} N_{\text{data}}^{\mathcal{R}}.$$

The control region  $\mathcal{R}$  is chosen away from the neutrino mass sensitive region so that the number of events expected in it does not depend strongly on the neutrino mass (see Fig. 2). The partial width is fit from an independent data sample as described in the text.



The event likelihood can be expanded as

$$\mathcal{L}_{\text{dat}}(\tilde{X}_{\text{data}}|\sigma_{\text{data}}, m_\nu, \bar{N}_{\text{bgd}}) = \left(1 - \frac{\bar{N}_{\text{bgd}}}{N_{\text{obs}}^\Omega}\right) \mathcal{L}_{\text{sig}}(\tilde{X}_{\text{data}}|\sigma_{\text{data}}, m_\nu) + \left(\frac{\bar{N}_{\text{bgd}}}{N_{\text{obs}}^\Omega}\right) \mathcal{L}_{\text{bgd}}(\tilde{X}_{\text{data}}|\sigma_{\text{data}}).$$

The first term of this expression is the neutrino mass likelihood for a pure signal. The second term expresses the background shape. The likelihoods  $\mathcal{L}_{\text{sig}}$  and  $\mathcal{L}_{\text{bgd}}$  are normalized over the fit region  $\Omega$  and neutrino mass. The notation  $\tilde{X}_{\text{data}}$  is to stress that we use the reconstructed (smeared) variables for the data.

The background likelihood,  $\mathcal{L}_{\text{bgd}}$ , is a parameterization of the background event distribution from the high tag-mass sample described in the text.

The signal likelihood,  $\mathcal{L}_{\text{sig}}$ , is determined from Monte Carlo simulations, taking into account detector smearing, the physics of tau decays, and initial state radiation effects. The analytic expression for this likelihood, as used in previous analyses (see for instance [22]), can be written as

$$\mathcal{L}_{\text{sig}}(\tilde{X}_{\text{data}}|\sigma_{\text{data}}, m_\nu) = \frac{\int_{\text{All } X} dX G(X, \tilde{X}_{\text{Data}}, \tilde{\sigma}_{\text{Data}}) \epsilon(X) f_{\text{Phys}}(X|m_\nu)}{\mathcal{N}(m_\nu)},$$

$$\mathcal{N}(m_\nu) = \int_{\Omega} d\tilde{X} \int_{\text{All } X} dX G(X, \tilde{X}, \tilde{\sigma}) \epsilon(X) f_{\text{Phys}}(X|m_\nu),$$

where

- $\tilde{X}$  is the reconstructed data point coordinate:  $(\tilde{M}, \tilde{E})$ ;
- $f_{\text{Phys}}(X|m_\nu)$  represents the physics, and is a convolution over the differential decay rate  $d\Gamma(m_\nu, X)/dq^2$ , and corrections due to initial state radiation, and beam energy smearing;
- $G(X, \tilde{X}, \sigma_{\text{data}})$ , a detector smearing function, is the probability of an observed  $\tilde{X}$  given a true  $X$  and an estimated error  $\sigma_{\text{data}}$ ;
- $\epsilon$  is the total detector efficiency.

Noting that Monte Carlo events are naturally generated with a probability density proportional to  $f_{\text{Phys}}$ , the signal likelihood for a given data event is rewritten as

$$\mathcal{L}_{\text{sig}}(\tilde{X}_{\text{data}}|\sigma_{\text{data}}, m_\nu) = \frac{\sum_{MC|m_\nu=0} G(\tilde{X}_{\text{data}}, X_{\text{MC}}, \sigma_{\text{data}}) \times \mathcal{W}(m_\nu|X_{\text{MC}})}{\mathcal{N}(m_\nu)}.$$

The sum is taken over all accepted Monte Carlo events, generated with a massless neutrino. The term  $\mathcal{W}(m_\nu|X_{\text{MC}})$  represents the relative weight of the Monte Carlo event for a massive neutrino compared to a massless neutrino. It is calculated at the generated  $(M, E)$  rather than the reconstructed  $(\tilde{M}, \tilde{E})$ , and is written as

$$\mathcal{W}(m_\nu|X_{\text{MC}}) = \frac{d\Gamma(m_\nu|X_{\text{MC}})}{d\Gamma(m_\nu=0|X_{\text{MC}})} \Theta(X_{\text{MC}}).$$

This is simply the ratio of differential decay rates of a tau at the (generated) value of  $q^2$  appropriate for this Monte Carlo event and this value of neutrino mass relative to a massless neutrino. Note that the matrix element factorizes and that the hadronic currents cancel in this ratio. The function  $\Theta$  ensures that only Monte Carlo events which remain physical at the new neutrino mass are used, and is implemented by checking that the scaled energy of the Monte Carlo event falls into the physically allowed interval

$$\Theta(X_{\text{MC}}) = \begin{cases} 1 & y_-(m_\nu) \leq \frac{E_X}{E_B} \leq y_+(m_\nu) \\ 0 & \text{else} \end{cases}.$$

The kinematic limits are given by

$$y_{\pm} = \frac{1}{2M_{\tau}^2} (E_{\tau}/E_B) \left( M_{\tau}^2 + q^2 - m_{\nu}^2 \pm \left( 1 - M_{\tau}^2/E_{\tau}^2 \right)^{\frac{1}{2}} \lambda^{\frac{1}{2}}(M_{\tau}^2, q^2, \nu^2) \right),$$

$$\lambda(x, y, z) = x^2 + y^2 + z^2 - 2(xy + yz + xz).$$

The factor  $\mathcal{N}(m_{\nu})$  ensures that the probability density used in the event likelihood is normalized for any neutrino mass:

$$\mathcal{N}(m_{\nu}) = \sum_{\text{MC}|m_{\nu}=0} \left( \int_{\Omega} G(\tilde{X}, X_{\text{MC}}, \sigma) d\tilde{X} \right) \mathcal{W}(m_{\nu}|X_{\text{MC}}).$$

The likelihood function used has been tested on Monte Carlo samples of decays with both massless and massive neutrinos and reproduces the input neutrino mass with no apparent bias.

## References

- [1] S.S. Gershtein, Ya.B. Zeldovich, JTEP Lett. 4 (1966) 174.
- [2] R. Cowsik, J. McClelland, Phys. Rev. Lett. 29 (1972) 669.
- [3] A.S. Szalay, G. Marx, Astron. and Astrophys. 49 (1976) 437.
- [4] E. Kolb, M. Turner, The Early Universe, Addison-Wesley, New York, 1990.
- [5] P.J.E. Peebles, Physical Cosmology, Princeton University Press, Princeton, 1993.
- [6] M. Kawasaki et al., Nucl. Phys. B 419 (1994) 105.
- [7] J.B. Rehm, G.G. Raffelt, A. Weiss, Astronomy and Astrophysics 327 (1997) 443.
- [8] ALEPH Collaboration, D. Buskulic et al., Phys. Lett. B 349 (1995) 585.
- [9] ALEPH Collaboration, R. Barate et al., CERN PPE/97-138, submitted to Z. Phys. C.
- [10] DELPHI Collaboration, A. Galloni, R. McNulty et al., A Limit on the Tau Neutrino Mass, submitted to HEP97, Jerusalem, 1997.
- [11] OPAL Collaboration, R. Akers et al., Z. Phys. C 72 (1996) 231.
- [12] OPAL Collaboration, R. Akers et al., Z. Phys. C 65 (1995) 183.
- [13] ARGUS Collaboration, H. Albrecht et al., Phys. Lett. B 202 (1988) 149.
- [14] ARGUS Collaboration, H. Schröder, Mod. Phys. Lett. A 8 (1993) 573.
- [15] CLEO Collaboration, D. Cinabro et al., Phys. Rev. Lett. 70 (1993) 3700.
- [16] CLEO Collaboration, Y. Kubota et al., Nucl. Instr. and Meth. A 320 (1992) 66.
- [17] S.J. Sojstrand, LUND 7.3, CERN-TH-6488-92, 1992.
- [18] R. Brun et al., GEANT v. 3.14, CERN Report No. CC/EE/84-1, 1987.
- [19] KORALB (v2.2)/TAUOLA (V2.4): S. Jadach, Z. Was, Comp. Phys. Com. 36 (1985) 191; 64 (1991) 267; S. Jadach, J.H. Kühn, Z. Was, Comp. Phys. Com. 64 (1991) 275; 70 (1992) 69; 76 (1993) 361.
- [20] E. Barbiero, B. van Eijk, Z. Was, CERN-TH-5857/90, 1990.
- [21] Particle Data Group, R.M. Barnett et al., Phys. Rev. D 54 (1996).
- [22] L. Passalacqua, Nucl. Phys. B (Proc. Suppl.) 55C (1997) 435.
- [23] Y.S. Tsai, Phys. Rev. D 4 (1971) 2821.
- [24] F. Gilman, D. Miller, Phys. Rev. D 17 (1978) 1846.
- [25] T.N. Pham, C. Roiesnel, T.N. Truong, Phys. Lett. B 78 (1978) 623.